# Asymmetric charge renormalization for nanoparticles in aqueous media

P. González-Mozuelos[1,2] and M. Olvera de la Cruz[1]
[1]*Department of Chemistry and Department of Materials Science and Engineering, Northwestern University, Evanston, Illinois 60208, USA*
[2]*Departamento de Física, Cinvestav del I. P. N., Avenida Instituto Politécnico Nacional 2508, Col. San Pedro Zacatenco, México, Distrito Federal, C. P. 07360, Mexico*

(Received 27 June 2008; revised manuscript received 19 January 2009; published 3 March 2009)

The effective renormalized charge of nanoparticles in an aqueous electrolyte is essential to determine their solubility. By using a molecular model for the supporting aqueous electrolyte, we find that the effective renormalized charge of the nanoparticles is strongly dependent on the sign of the bare charge. Negatively charged nanoparticles have a lower effective renormalized charge than positively charged nanoparticles. The degree of asymmetry is a nonmonotonic function of the bare charge of the nanoparticle. We show that the effect is due to the asymmetric charge distribution of the water molecules, which we model using a simple three-site molecular structure of point charges.

DOI: 10.1103/PhysRevE.79.031901 PACS number(s): 87.19.rf, 61.20.Gy, 61.20.Qg, 77.22.−d

## I. INTRODUCTION

Electrostatic interactions control important biological and biotechnological processes. They also play a key role in the properties of molecular liquids of industrial interest. In particular, electrostatic interactions are essential for understanding new discoveries associated with assemblies of charged nanoparticles with biomolecules and their interactions with cells [1,2]. The solubility of charged nanoparticles in electrolyte solutions is also crucial for developing new drugs and for drug delivery [3]. Moreover, charged nanoparticles are added to colloidal suspensions to stabilize them against macroscopic segregation via the phenomenon known as haloing [4–7].

The solubility of charged particles in aqueous solutions is strongly dependent on their effective renormalized charge. As a rule, the stronger the reduction of charge of the particles, the higher their solubility in simple electrolytes. The charge of macroions, including proteins and nucleic acids as well as nanoparticles and microspheres, is renormalized by the small ions [8] and the polar solvent molecules [9]. The effective renormalized charge of molecules, such as proteins which expose the charges at their surface, can be inferred by physical techniques including capillary electrophoresis [10] and vibrational spectroscopy [11]. Moreover, new experiments that allow the direct observation of charged nanoparticles [12] may provide information about their effective renormalized charges.

The effective interactions among suspended nanoparticles have been extensively studied with models that ignore the molecular structure of the supporting electrolyte. For example, the correlations among charged spherical particles (macroions) suspended in a simple electrolyte are typically computed using the Derjaguin-Landau-Verwey-Overbeek (DLVO) model pair potential, which basically consists of hard sphere plus screened electrostatic (Yukawa) potentials [13,14]. In this and related models the solvent is assumed to be a structureless continuum with the effective dielectric constant of water. Therefore the structure of water near the charged surfaces and the contrast of the permittivities inside and outside the macroions are ignored. These effects are expected to strongly influence the effective interactions among dissolved nanoparticles since even in the vicinity of uncharged surfaces water has strong conformational changes [15]. Despite its importance, there are no models that predict the solubility of simple charged nanoparticles in aqueous solutions.

There have been many studies of ions in water. Their solubility is associated with their size via the Born model [16]. However, results regarding charge asymmetry of macromolecules cannot be described with simple models. It has been known for a long time that proteins have different solubilities in the presence of different ions [17], which is believed to be due to strongly specific charge renormalization of the proteins. Indeed, partitioning of the salt ions between the bulk and the interface of the molecules is observed to be ion specific for various macromolecules [11]. In order to understand this partitioning, models that include the water explicitly are required. There are no studies of the effective renormalized charge of even simple spherical nanoparticles that include water because of the enormous difficulties associated with modeling such a large number of molecules with long ranged Coulomb interactions.

By using a model that introduces the molecular structure of a waterlike polar solvent, we show here that even when the small ionic components are assumed to be pointlike, the spherical nanoparticles have strongly asymmetric renormalized charges. The negatively charged nanoparticles are effectively less charged than the positive ones, and the degree of asymmetry depends on the size and the bare charge of the nanoparticles. Our results suggest that in the absence of short ranged attractions among nanoparticles, positively charged nanoparticles have larger solubility than negatively charged nanoparticles. Dipolar interactions were recently included in electrolytes in contact with flat surfaces using a mean field model [18]. Here we instead consider charges separated by rigid bonds to be able to represent the electrolyte molecular structure.

Here we study the effect of the asymmetric charge distribution of the water molecules on the effective renormalized charges of the nanoparticles by applying the dressed interac-

 

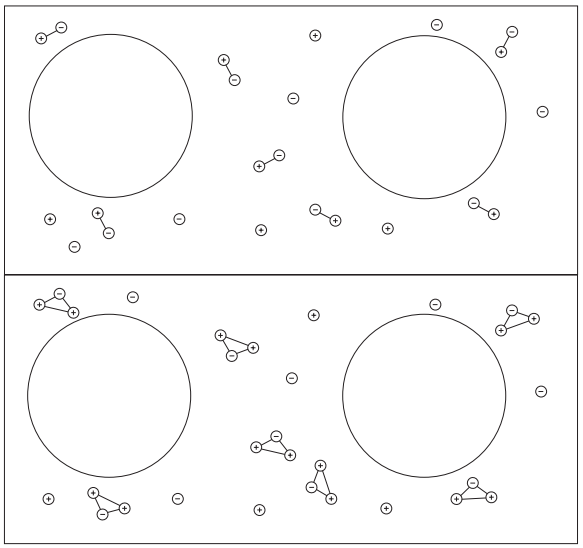

FIG. 1. The model systems: symmetric solvent molecules in the upper panel; waterlike solvent molecules in the lower panel. The densities of solvent molecules and relative sizes are not correctly represented.

tion site theory (DIST) [9,19–22]. This model gives the effective pair potentials among nanoparticles, which are in turn obtained from the two-point correlations of the whole model system. Like in the approaches using the primitive model (PM) as the starting point [8,23], our goal is to derive the pair potentials that generate the same total correlation functions among the macroions. We have calculated these interactions in systems with larger size asymmetries assuming that the solvent molecules are rodlike molecules with opposite point charges at their ends [9]. In this work we also consider a second model for the solvent molecules [19] where three point charges (sites) connected by rigid rods, one oxygen site plus two hydrogen sites, represent the water molecules. Both model systems also include the spherical macroions at infinite dilution and point salt ions at finite concentration. The schematics of both model systems (not at scale, neither in sizes nor densities) are shown in Fig. 1. The effective renormalized charge including the structure of the solvent is less than the one computed assuming a structureless solvent. By comparing the two models for the structure of the solvent shown in Fig. 1, we find that besides permittivity contrast, the shape and charge distribution of the solvent molecules also contribute to the charge renormalization of the macroions. The asymmetry in the effective renormalized charge of the positive and negatively charged nanoparticles found here with the model shown in the lower panel in Fig. 1 is a nontrivial function of the nanoparticle size and bare charge.

## II. THEORY

We apply a reference interaction site model (RISM) approach for the description of both model systems, each constituted by five different species of interaction sites. The three ionic species on both models are the small anions, denoted by subindex $a$, the small cations, denoted by $c$, and the macroions, denoted by $M$. Besides these ions we also have the interaction sites of the solvent molecules. In the first model each solvent molecule has one positive site, denoted as species $p$, and one negative site, denoted as species $n$. In the second model each solvent molecule has one negative site, belonging to species $O$, and two positive sites, both belonging to species $H$. The pair potentials among all the interaction sites are of the form

$$\beta u_{ij}(r) = \beta u_{ij}^{HS}(r;\sigma_{ij}) + \frac{l_b}{r}[1-\exp(-\alpha r)]q_i q_j, \qquad (1)$$

for $i,j=M,a,c,p,n,O,H$, where $\beta \equiv 1/k_B T$, $k_B$ is Boltzmann's constant, $T$ is the temperature of the system, $l_b \equiv \beta e^2/4\pi\epsilon_r\varepsilon_0$ is Bjerrum's length, $e$ is the proton charge, $\varepsilon_0$ is the dielectric constant of the vacuum, $\epsilon_r$ is the relative dielectric constant of the background, and $q_i$ is the electric charge of an interaction site of species $i$ in proton units. The short-range component of the interaction is the hard sphere potential with $\sigma_{ij}=(\sigma_i+\sigma_j)/2$, $\sigma_i$ being the diameter of species $i$. In the present work $\sigma_i=0$ for the species in the supporting electrolyte, that is, for $i=a$, $c$, $p$, $n$, $O$, and $H$. Thus only the macroions have finite size ($\sigma_M>0$). Since $\beta u_{ij}(0) = l_b \alpha q_i q_j$ when $\sigma_{ij}=0$, the parameter $\alpha^{-1}$ acts as the "effective" diameter of the interacting sites in the supporting electrolyte. Here we use the value $\alpha^{-1}=0.32$ nm.

In these interaction site models the total correlation functions are expressed as the sum of intramolecular and intermolecular components: $h_{ij}(r)=h_{ij}^0(r)+h_{ij}^a(r)$. These components are related to the direct intermolecular correlation functions $c_{ij}^a(r)$ by the RISM equation, which in Fourier space takes the form

$$\rho_i \tilde{h}_{ij}^a(k)\rho_j = \sum_{p=1}^{M}\sum_{r=1}^{M} \tilde{\omega}_{ip}(k)\tilde{c}_{pr}^a(k)[\tilde{\omega}_{rj}(k)+\rho_r \tilde{h}_{rj}^a(k)\rho_j], \qquad (2)$$

where $\tilde{\omega}_{ij}(k) \equiv \rho_i \delta_{ij} + \rho_i \tilde{h}_{ij}^0(k)\rho_j$, $M$ is the number of species of interaction sites in the system, and $\rho_i$ is the number density of interaction sites of species $i$. One of the main results from the DIST is that total correlation functions take the general rigorous form

$$\tilde{h}_{ij}^a(k) = \tilde{h}_{ij}^{sa}(k) - \tilde{z}_i^*(k) l_b \tilde{v}^*(k) \tilde{z}_j^*(k), \qquad (3)$$

where the functions $\tilde{h}_{ij}^{sa}(k)$ and $\tilde{c}_{ij}^{sa}(k) \equiv \tilde{c}_{ij}^a(k) + 4\pi l_b q_i q_j \alpha^2/(k^2+\alpha^2)k^2$ are connected by RISM-like equations, and the renormalized charge distributions and electrostatic potential, $\tilde{z}_i^*(k)$ and $\tilde{v}^*(k)$, respectively, are related to the bare charge distributions and electrostatic potential by a set of well defined relations that also involve $\tilde{h}_{ij}^{sa}(k)$ [20,21]. From this general result follows that the asymptotic behavior of the total intermolecular correlation functions has, for sufficiently low ionic concentrations, the general form

$$h_{ij}^{a}(r) \sim -\frac{l_b}{E^* r}\exp(-\eta r) q_i^* q_j^*, \tag{4}$$

where the inverse screening length $\eta$ is related mainly to the ionic strength of the solution, the renormalized dielectric constant $E^*$ is mostly generated by the polarizability of the solvent, and the effective renormalized charge $q_i^*$ strongly depends on both effects. Likewise, the effective pair potential between two macroions has an electrostatic component of the form

$$\beta \tilde{u}_{ij}^{ee}(k) = \tilde{z}_i^{(r)}(k) l_b \tilde{v}^{(r)}(k) \tilde{z}_j^{(r)}(k), \tag{5}$$

where $i$ and $j$ now correspond to species in the observable subset. The expressions for the effective renormalized charge distributions and electrostatic potential appearing in this last equation have been presented before [20,22]. Thus the asymptotic form of this effective pair potential is also of the Yukawa-like form [9,19,20,22]

$$\beta u_{MM}^{eff}(r) \sim \frac{l_b}{E^{(r)} r}\exp(-\kappa r) a_M^2, \tag{6}$$

and in the limit of $\rho_M = 0$ we get that $a_M = q_M^*$ for the effective renormalized charge, $\kappa = \eta$ for the effective screening length, and $E^{(r)} = E^*$ for the effective dielectric constant. The asymptotic forms given in Eqs. (4) and (6) do not correspond to an effective background medium or "averaged solvent," they represent general results, valid for any microscopic model, and have also been derived within the dressed molecule theory developed by Ramirez and Kjellander [24,25].

## III. RESULTS AND DISCUSSION

For the first model system we have that $\tilde{h}_{pn}^0(k) = \tilde{h}_{np}^0(k) = j_0(l_w k)/\theta_w$, where $\theta_w$ is the number density of solvent molecules, so $\rho_p = \rho_n = \theta_w$, and $l_w$ is the distance between the positive and negative sites within the same solvent molecule. For the second model system, on the other hand, we have that $\tilde{h}_{HH}^0(k) = j_0(l_{HH}k)/2\theta_w$, $\tilde{h}_{HO}^0(k) = \tilde{h}_{OH}^0(k) = j_0(l_{OH}k)/\theta_w$, and $\tilde{h}_{OO}^0(k) = 0$, so in this case $\rho_H = 2\rho_O = 2\theta_w$, and $l_{HH}$ and $l_{OH}$ are, respectively, the distances between the two hydrogen sites and between each hydrogen site and the oxygen site within each water molecule. In both models all the other intramolecular correlation functions are null and the background is the vacuum, so $\epsilon_r = 1$ and $l_b = 56.0$ nm at room temperature. We also take $\theta_w = 33.45$ nm$^{-3}$, which corresponds to the number density of water molecules at standard conditions. The remaining parameters of both models are adjusted to fit the effective dielectric constant of Eq. (6) to the experimental value at standard conditions: $E^{(r)} = 78$. For the first model this is attained with the values $l_w = 0.1$ nm and $q_p = -q_n = 1$, which are typical (but arbitrary) values for molecular solvents [9]. For the second model, we take the values $l_{HH} = 0.15$ nm, $l_{OH} = 0.0975$ nm, which closely resemble the experimental data on water molecules; the sites charges are set to $q_O = -2q_H = -1.594$ to get the appropriate $E^{(r)}$ [19].

Here we consider the infinite macroion dilution limit $\rho_M = 0$ and assume a monovalent added salt: $q_a = -q_c = -1$. The hypernetted-chain (HNC) closure is used for all the correlation functions between a macroion and any other component, whereas the random phase approximation (RPA) closure is used for all the other correlations. The set of integral equations obtained from the real space version of Eq. (2), complemented with these closures, is then solved with the same numerical method previously used [9], which allows us to explore a wide range of values for $\sigma_M$ and $q_M$. Figures 2–4 illustrate the results for the ratio of the macroion effective renormalized charge to its bare charge, $a_M/q_M$, as a function of $q_M$ for different salt concentrations and macroion diameters. The white circles correspond to the model with symmetric solvent molecules and the black squares correspond to the waterlike solvent.

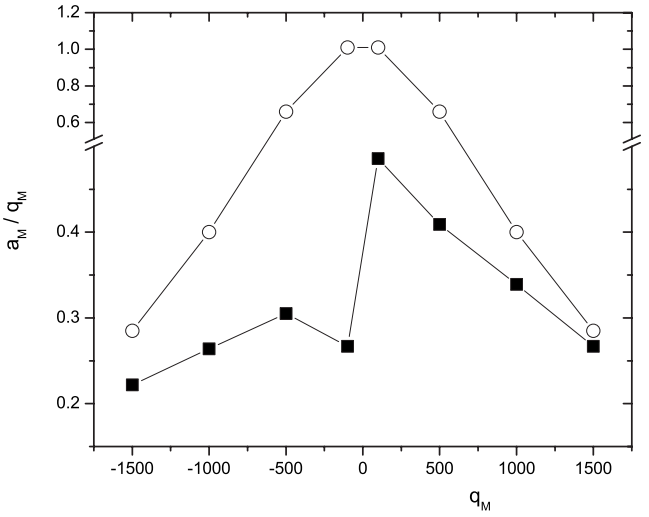


FIG. 2. Ratio of the effective renormalized charge $a_M$ to the bare charge $q_M$ as a function of $q_M$ for $\sigma_M = 30$ nm and $\rho_a = \rho_c = 0.001$ M. The white circles correspond to the model with symmetric solvent molecules and the black squares correspond to the waterlike solvent.

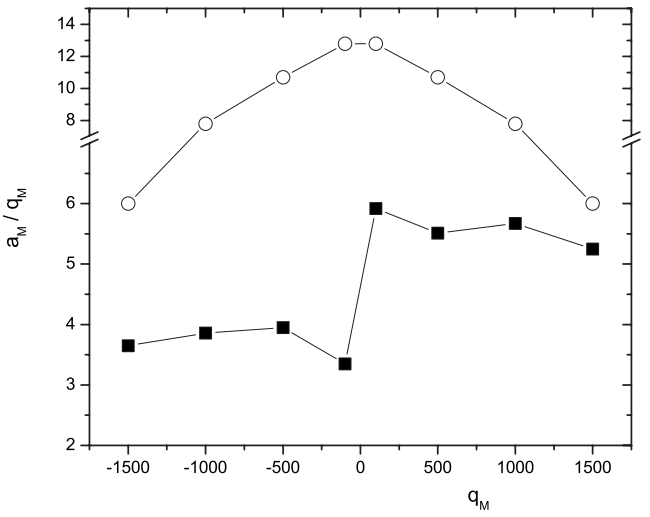


FIG. 3. Ratio of the effective renormalized charge $a_M$ to the bare charge $q_M$ as a function of $q_M$ for $\sigma_M = 30$ nm and $\rho_a = \rho_c = 0.01$ M. The white circles correspond to the model with symmetric solvent molecules and the black squares correspond to the waterlike solvent.

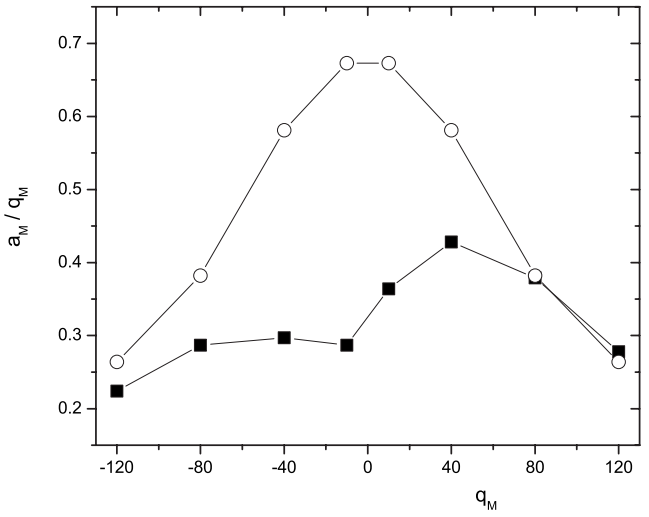


FIG. 4. Ratio of the effective renormalized charge $a_M$ to the bare charge $q_M$ as a function of $q_M$ for $\sigma_M$=6 nm and $\rho_a$=$\rho_c$=0.001 M. The white circles correspond to the model with symmetric solvent molecules and the black squares correspond to the waterlike solvent.

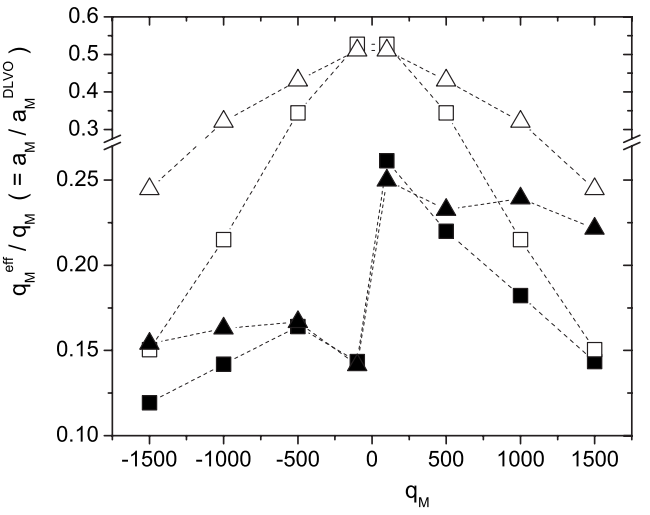


FIG. 5. Ratio of the effective charge $q_M^{eff}$ given in Eq. (8) to the bare charge $q_M$ (or, equivalently, of the renormalized charge $a_M$ to the corresponding DLVO value $a_M^{DLVO}$) as a function of the bare charge $q_M$. The white symbols correspond to the model with symmetric solvent molecules and the black symbols correspond to the waterlike solvent. The squares correspond to $\sigma_M$ =30 nm and $\rho_a$ =$\rho_c$=0.001 M. The triangles correspond to $\sigma_M$ =30 nm and $\rho_a$ =$\rho_c$=0.01 M.

It is also interesting to compare these results against those corresponding to the DLVO theory [14], where the electrostatic component of the pair potential has the same form of Eq. (6) but with an effective charge given by

$$\frac{a_M^{DLVO}}{q_M} = \frac{\exp(\kappa\sigma_M/2)}{1+\kappa\sigma_M/2}. \tag{7}$$

In this theory the solvent is not explicitly taken into account, it only appears as a background dielectric constant, and the mean spherical approximation (MSA) is used for the determination of the correlations between the macroion and the point ions [while taking $\alpha^{-1}$=0 in Eq. (1)]. The expression in Eq. (7) was also used by Alexander and collaborators [8] to introduce the definition of an effective charge $q_M^{eff}$ that is slightly different from the one used here. Thus this DLVO-effective charge is in essence given by

$$q_M^{eff} = \frac{a_M}{a_M^{DLVO}} q_M, \tag{8}$$

where $a_M$ is the effective renormalized charge defined in Eq. (6) and reported in Figs. 2–4. The comparison between $a_M$ and $a_M^{DLVO}$ is then equivalent to the comparison between $q_M^{eff}$ and $q_M$.

Figures 2 and 3 correspond to a nanoparticle of size $\sigma_M$ =30.0 nm. In Fig. 2 the salt concentration is $\rho_a$=$\rho_c$ =0.001 M=6.022×$10^{-4}$ $nm^{-3}$, for which the screening length is $\kappa^{-1}$=9.6 nm and the corresponding DLVO value is $a_M^{DLVO}/q_M$=1.86. A higher salt concentration, $\rho_a$=$\rho_c$ =0.01 M, is illustrated in Fig. 3, so in this case $\kappa^{-1}$ =3.0 nm and $a_M^{DLVO}/q_M$=23.7. The magnitude of the effective renormalized charges in the two models studied here is clearly smaller than the corresponding DLVO value, and this effect is more marked when the magnitude of the bare charge increases, which is in agreement with previous findings [8] (i.e., $q_M^{eff} < q_M$). Furthermore, the model with symmetric solvent consistently predicts larger magnitudes of the renormalized charge in comparison to the one with waterlike solvent. But the most salient feature of this last model is the asymmetric charge renormalization in regard to the bare macroion charge: a positive value of $q_M$ induces a larger magnitude of $a_M$ than a negative value of $q_M$, more markedly for smaller values of the magnitude of the bare charge. Under the conditions of Fig. 2, for example, we have that $a_M$=−26.7 for $q_M$=−100, whereas $a_M$=48.6 for $q_M$=100.0, and therefore $|a_M(q_M=100)/a_M(q_M=-100)|$=1.82.

These effects are still present, though somehow diminished, at smaller macroion sizes. Figure 4 shows the data for $\sigma_M$=6 nm and $\rho_a$=$\rho_c$=0.001 M, for which $a_M^{DLVO}/q_M$=1.04 (so again $a_M < a_M^{DLVO}$, i.e., $q_M^{eff} < q_M$, for both models with explicit solvent). In this case the charge renormalization differences between symmetric and waterlike model solvents are almost negligible for $q_M \geqslant 80$, and the charge asymmetry in the waterlike solvent model is also less marked here than in the case with larger macroions. In this case, for example, the largest asymmetry corresponds to $|a_M(q_M=40)/a_M(q_M=-40)|$=1.44.

In the literature, the DLVO-effective charge defined by Eq. (8) is often used to compare with experimental results [8]. In order to compare our results with previous models where the solvent is structureless [8], we plot in Figs. 5 and 6 the ratio of this DLVO-effective charge to the bare charge versus the bare charge and versus the bare surface charge density, respectively. In Fig. 5 we plot the DLVO-effective charge to bare charge ratio versus the bare charge for two different salt concentrations for nanoparticles of diameter $\sigma_M$ =30 nm. As expected, the DLVO-effective charge is more renormalized at low salt concentrations and the ratio of the effective charge $q_M^{eff}$ to the bare charge $q_M$ is less than 1. We

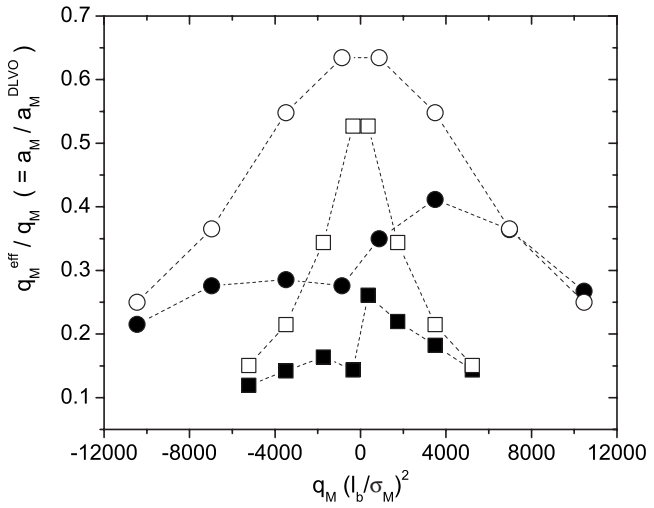


FIG. 6. Ratio of the effective charge $q_M^{eff}$ given in Eq. (8) to the bare charge $q_M$ as a function of the dimensionless bare charge surface density $q_M(l_b/\sigma_M)^2$. The white symbols correspond to the model with symmetric solvent molecules and the black symbols correspond to the waterlike solvent. The squares correspond to $\sigma_M$ =30 nm and $\rho_a=\rho_c=0.001$ M. The circles correspond to $\sigma_M$ =6 nm and $\rho_a=\rho_c=0.001$ M.

note that the DLVO-effective charge when the structure of the solvent is included, is always less than the value computed when the solvent is a structureless medium. Moreover, the structured waterlike solvent yields low and nonsymmetric DLVO-effective charges. The degree of asymmetry in the DLVO-effective charge of nanoparticles is a nonmonotonic function of the bare charge, and it decreases as the salt concentration increases.

In Fig. 6 we plot the ratio of the DLVO-effective charge to the bare charge as a function of the dimensionless bare charge surface density $q_M(l_b/\sigma_M)^2$ for two different nanoparticle sizes. This figure clearly shows that the DLVO-effective charge is a nontrivial function of the bare surface charge density: the large nanoparticles seem to have lower DLVO-effective charge than the small nanoparticles. Also, the maximum degree of asymmetry occurs at smaller values of the bare surface charge density in the larger nanoparticles than in the smaller nanoparticles. It will be interesting to determine in the future the degree of asymmetry when the nanoparticles reach micron sizes.

## IV. CONCLUDING REMARKS

The difference between the permittivities inside and outside the macroions contributes to the noticeable reduction of the magnitude of the effective renormalized charge $a_M$ when compared to the magnitude of the corresponding DLVO value. Thus the approach discussed here seems to indicate that the image charge effect is present even for such small nanoparticles. In certain limits it is possible to show that integral equation approaches generate the same results of conventional methods such as the Poisson-Boltzmann equations methods [26–28]. Although it is hard to show analytically that the charge renormalization from our approach contains the image charge effect, one can understand this effect by comparing our results for the structured solvent molecules, where the nanoparticles have a local dielectric constant inside approximately equal to 1 and outside approximately equal to 80, with the results of a model where the solvent is not included explicitly so the dielectric constants inside and outside the nanoparticles are the same [9]. The charge is more renormalized in the systems with explicit solvent molecules than in the system without solvent molecules. The counterion image charges are known to reduce the effective macroion charge, while the coions produce the opposite effect. Since screening affects more the more distant coions from the nanoparticles, the counterion charge images contribution dominates leading to a reduced effective macroion charge. This effect becomes less important as the charge of the macroions increases since in that case the nonlinear character of the approach (discussed by Alexander *et al.* [8]) overrides the permittivity differences, though indeed both contributions lead to $a_M < a_M^{DLVO}$, and therefore $q_M^{eff} < q_M$.

Our results indicate the presence of other effects besides permittivity contrast. That is, the particular shape and charge distribution of the solvent molecules also contribute to the charge renormalization of the macroions. Since both solvent structured model systems neglect the repulsive core and short ranged attractions in the interactions among the solvent molecules, the asymmetric charge renormalization described here is mostly due to the configurational constrains on the orientations of the solvent molecules in the vicinity of the macroions, and the ensuing effects on their entropic contribution. This is not surprising since water orientation has been observed with simulations of water with hydrophobic (uncharged) flat interfaces [29]. The effect, however, is not trivial in the presence of surface and bulk charges since there is a maximum charge renormalization asymmetry at intermediate bare charges of the nanoparticles. Moreover, when the DLVO-effective charge is plotted versus the bare surface charge density of nanoparticles, it is obvious that the degree of asymmetry occurs at different surface charge densities values for different nanoparticles sizes. Our approach suggests that there are subtle competitive effects in these systems. More realistic models of the polar solvent molecules [20,22] should clarify the underlying mechanisms of this nonmonotonic macroion charge renormalization asymmetry.

Our work has significant consequences to the thermodynamics of charged nanoparticles in aqueous media. For example, the water electrolyte model used here generates charge asymmetric interactions between nanoparticles, which may lead to charge asymmetric phase diagrams, as seen in phase diagrams using phenomenological asymmetric interactions in a continuum medium [30]. For such studies extension of molecular models that treat confinement of water [31] and charges [32] are required. Moreover, we expect that extensions of our model to complex nanoparticle structures explain some of the anomalies observed in the Hofmeister series [11,17] regarding the solubility of proteins. The charge polarizability of the nanoparticles, when significant, is expected to modify the charge renormalization. It should be of interest to compare the degree of charge renormalization asymmetry of charged rodlike chains with spherical nanoparticles of equal magnitude of bare charge in structured solvents.

**ACKNOWLEDGMENTS**

This work was financially supported by Conacyt-Mexico under Grants No. SEP-2006-U1-60595 and No. SEP-2006-C1-49486, by NSF under Grant No. DMR 0520513, and by DOE under Grant No. DE-FG02–08ER46539. M.O. thanks J. Rodgers for useful suggestions.

[1] I. Lynch, T. Cedervall, M. Lundqvist, C. Cabaleiro-Lago, S. Linse, and K. A. Dawson, Adv. Colloid Interface Sci. **134-135**, 167 (2007).
[2] D. A. Giljohann, D. S. Seferos, P. C. Patel, J. E. Millstone, N. L. Rosi, and C. A. Mirkin, Nano Lett. **7**, 3818 (2007).
[3] W. L. Jorgensen and E. M. Duffy, Adv. Drug Delivery Rev. **54**, 355 (2002).
[4] C. J. Matinez, J. Liu, S. K. Rhodes, E. Luijten, E. R. Weeks, and J. A. Lewis, Langmuir **21**, 9978 (2005).
[5] M. Chávez-Páez, P. González-Mozuelos, M. Medina-Noyola, and J. M. Méndez-Alcaraz, Physica A **341**, 1 (2004).
[6] J. Liu and E. Luijten, Phys. Rev. E **72**, 061401 (2005).
[7] E. N. Scheer and K. S. Schweizer, J. Chem. Phys. **128**, 164905 (2008).
[8] S. Alexander, P. M. Chaikin, P. Grant, G. J. Morales, and P. Pincus, J. Chem. Phys. **80**, 5776 (1984).
[9] P. González-Mozuelos and M. Olvera de la Cruz, Physica A **387**, 5362 (2008).
[10] I. Gitlin, J. D. Carbeck, and G. M. Whitesides, Angew. Chem., Int. Ed. **45**, 3022 (2006).
[11] X. Chen, T. Yang, S. Kataoka, and P. S. Cremer, J. Am. Chem. Soc. **129**, 12272 (2007).
[12] F. Zhang, G. G. Long, P. R. Jemian, J. Ilavsky, V. T. Milam, and J. A. Lewis, Langmuir **24**, 6504 (2008).
[13] E. J. W. Verwey and J. Th. G. Overbeek, *Theory of the Stability of Lyophobic Colloids* (Elsevier, Amsterdam, 1948).
[14] W. B. Russel, D. A. Saville, and W. R. Schowalter, *Colloidal Dispersions* (Cambridge University Press, Cambridge, England, 1989).
[15] L. Maibaum and D. Chandler, J. Phys. Chem. B **111**, 9025 (2007).
[16] R. W. Gurney, *Ionic Processes in Solution* (Dover, New York, 1962).
[17] F. Hofmeister, Naunyn-Schmiedeberg's Arch. Pharmacol. **24**, 247 (1888).
[18] A. Abrashkin, D. Andelman, and H. Orland, Phys. Rev. Lett. **99**, 077801 (2007).
[19] P. González-Mozuelos and N. Bagatella-Flores, Physica A **286**, 56 (2000).
[20] N. Bagatella-Flores and P. González-Mozuelos, J. Chem. Phys. **117**, 6133 (2002).
[21] P. González-Mozuelos, M. S. Yeom, and M. Olvera de la Cruz, Eur. Phys. J. E **16**, 167 (2005).
[22] P. González-Mozuelos, J. Phys. Chem. B **110**, 22702 (2006).
[23] P. González-Mozuelos and M. D. Carbajal-Tinoco, J. Chem. Phys. **109**, 11074 (1998).
[24] R. Ramirez and R. Kjellander, J. Chem. Phys. **119**, 11380 (2003).
[25] R. Ramirez and R. Kjellander, J. Chem. Phys. **125**, 144110 (2006).
[26] M. Lozada-Cassou and D. Henderson, Chem. Phys. Lett. **127**, 392 (1986).
[27] M. Lozada-Cassou and E. Díaz-Herrera, J. Chem. Phys. **93**, 1386 (1990).
[28] P. González-Mozuelos and M. Olvera de la Cruz, J. Chem. Phys. **103**, 3145 (1995).
[29] C. Y. Lee, J. A. McCammon, and P. J. Rossky, J. Chem. Phys. **80**, 4448 (1984).
[30] W. Kung and M. Olvera de la Cruz, J. Chem. Phys. **127**, 244907 (2007).
[31] J. M. Rodgers and J. D. Weeks, Proc. Natl. Acad. Sci. U.S.A. **105**, 19136 (2008).
[32] J. M. Rodgers and J. D. Weeks, J. Phys.: Condens. Matter **20**, 494206 (2008).